Journal of Materials and Environmental Sciences
ISSN : 2028-2508
CODEN : JMESCN

J. Mater. Environ. Sci., 2019, Volume 10, Issue 6, Page 495-509

http://www.jmaterenvironsci.com

Effect of *Dialium guineense* extracts on the corrosion inhibition of aluminum in alkaline solutions

L. N. Emembolu,[*1] O. D. Onukwuli [2]

[*1,2]*Department of Chemical Engineering, Nnamdi Azikiwe University, Awka, Nigeria*

Received 08 May 2019,
Revised 20 June 2019,
Accepted 21 June 2019

Keywords
- ✓ *Dialium guineense*,
- ✓ Thermodynamics,
- ✓ Electrochemistry,
- ✓ Adsorption isotherm,
- ✓ Alkaline solutions.

lovethembolu@gmail.com

Abstract

The inhibiting effect of *Dialium guineense* extract on Aluminum corrosion in 3 M KOH and 3 M NaOH solutions were studied using gravimetric and electrochemical techniques at 303K, 323K, and 343K. The results obtained indicated that *Dialium guineense* extracts retarded the corrosion reaction in both alkaline media and inhibition efficiency increases as the extract concentration increases. The thermodynamics properties like Activation energy, heat of adsorption, enthalpy and entropy of adsorptions and Gibb's free energy were also calculated. Polarization curves demonstrated that the leaf extract were mixed-type inhibitors. EIS plots indicated that the addition of the extract increases the charge-transfer resistance of the corrosion process, and hence the inhibition performance.

1. Introduction

Alkaline solutions are used to control pH in aqueous solutions and is effective in breaking down organic matters. In water-based mud or drilling fluids, it increases and maintains alkalinity and pH levels [1]. The exposure of various metals to different aggressive environments like alkaline solutions by human activities created an avenue for metals to undergo different types of corrosion mechanisms. Mitigation of this corrosion is of the greatest challenges facing the world at present. This is because the impact of corrosion has created a huge loss in the economy of all countries as a whole, industries and even in our different homes [1-3].

Aluminum as a metal is important due to its properties of lightweight, strength, recyclability, corrosion resistance, durability, ductility, formability, and conductivity. These qualities earned Aluminum a wide range of applications in almost all the industries. Aluminum is resistant to corrosion as a result of the formation of the thin oxide film which prevents it from oxidation on exposure to the atmosphere [3]. However, it is possible for Aluminum to corrode if this protective film is destroyed or tampered with [4]. The pickling of Aluminum in caustic alkalis for degreasing before anodizing to give an attractive finish is common practice [3-6]. Alkalis destroy the protective aluminum film very fast because OH- ions are positively adsorbed [7], hence dissolution of aluminum is very high.

Nowadays, the development of modern society and industry has led to stronger demand for nontoxic, natural and environmental friendly inhibitors are required to mitigate the corrosion of aluminum in alkaline/acid media [8-14]. However, in this study, *Dialium guineense* leaves extracts with English name velvet tamarind was used to retard the corrosion inhibition of aluminum in alkaline solutions using weight loss and electrochemical method. The effect of temperature on the corrosion rate of aluminum with and without inhibitor was examined, adsorption and thermodynamic parameters were calculated and discussed in detail.

2. Material and Methods

2.1. Material preparation

Test were carried on Aluminum sheets with weight percentage composition as follows: Si (0.25%), Fe (0.02%), Zn (0.05%), Mn (0.04%) Mg (0.03%), V (0.04%), Ti (0.02%), Cu (0.03%), Cr (0.02%), and the balance Al. Each sheet, which was 0.16cm in thickness was mechanically pressed-cut into coupons of 5 x 4cm. These were used as a source without further polishing but were however degreased in absolute ethanol, dried in acetone and stored in a moisture-free desiccator prior to use. All chemicals and reagents used were analytical grades. The blank corrodents were respectively 3 M KOH and 3 M NaOH solutions. Stock solutions of the plant extract were prepared by boiling weighed amounts of the dried and ground leaves of Dialium guineense for 3 hours in 3 M KOH and 3 M NaOH solutions, respectively. The resulting solutions were cooled, then filtered and stored. From the respective stock solutions, inhibitor test solutions were prepared in the concentration range 0.2 – 1.0g/l.

2.2. Weight loss measurement

The Al sheets were abraded with different emery papers (grade 200, and 400), washed with double distilled water, rinsed with ethanol and acetone, and then dried at room temperature. After weighing accurately, the specimens were immersed in beakers containing 250 ml of 3 M KOH and 3 M NaOH solutions respectively with different concentrations of the tested inhibitors for 1, 2, 4, 6 and 8hr at 303 – 343K. After each immersion time, the specimens were taken out, washed, dried, and weighed accurately. In order to obtain good reproducibility, experiments were carried out in triplicate. The corrosion rate (Cr), surface coverage and inhibition efficiency (η%) were calculated from the following Eqs. (1)–(3) [15–17]:

$$Cr = \frac{W_0 - W_1}{ST} \quad (1)$$

$$\theta = \frac{W_0 - W_1}{W_0} \quad (2)$$

$$\eta\% = \frac{W_0 - W_1}{W_0} \times 100 \quad (3)$$

Where W_o and W_1 are the weight loss values in absence and presence of inhibitor, respectively, S is the total area per cm^2 and T is the immersion time in hr.

2.3. Potentiodynamic polarization measurements

Potentiodynamic polarization measurements were conducted using a Volta Lab-PGZ-301 (France). A conventional cylindrical glass cell of 250 mL with three electrodes was used. A platinum sheet of 2 cm^2 area and saturated calomel electrode (SCE) were used as auxiliary and reference electrodes, respectively. The working electrode was cut in the form of a disc (from the used Al) with an area of 0.8 cm^2 was embedded with epoxy except for the working surface. Potentiodynamic polarization curves were obtained by varying the potential automatically from -200 to +200 mV against the open circuit potential (OCP) with the scan rate of 2 mV s^{-1}. The inhibition efficiency (η%) was calculated using Eq. (4) as follows [18, 19];

$$\eta\% = \frac{i_{corr(uninh)} - i_{corr(inh)}}{i_{corr(inh)}} \times 100 \quad (4)$$

where $i_{corr(uninh)}$ and $i_{corr(inh)}$ are the corrosion current density values without and with inhibitors.

2.4. Electrochemical impedance spectroscopy measurements (EIS)

The electrochemical experiment was conducted in a three-electrode corrosion cell (as shown in Figure1) using a VERSASTAT 300 complete dc voltammetry and corrosion system with V3 studio software for electrochemical impedance spectroscopy and Potentiodynamic/Galvanstat corrosion system with E-chem software for Potentiodynamic polarization experiments. A graphite rod was used as a counter electrode and a saturated calomel

electrode (SCE) was used as reference electrode. The latter was connected via a plugging capillary. Impedance measurement was performed in aerated and unstirred solutions at the end of 1800 sat 30 ± 1°C. Impedance measurements were made at corrosion potentials (E_{corr}) over a frequency range of 100KHz - 0.1Hz with a signal amplitude perturbation of 5 mV [19]. An electrical equivalent circuit for the system is shown in Figure 1.

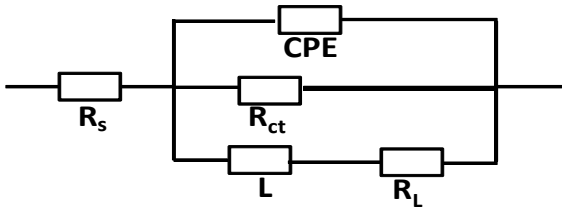

Figure 1: Equivalent circuit for impedance measurements

3. Results and discussion

3.1 Weight loss measurements, Corrosion rate and Inhibition efficiency

The values of the corrosion rate and inhibition efficiencies in absence and presence of different concentrations of the inhibitor (0.2, 0.4, 0.6, 0.8 and 1.0g/L) were obtained from weight loss measurements using Eqs. (1) – (3) at 303, 323 and 343K respectively and were listed in Table 1. Figures 2(a) and (b) indicate the weight loss versus time for the corrosion behavior of Al in 3 M KOH and 3 M NaOH solution containing *D. guineense* within the concentration range of 0.2 –1.0 g/L. The plot reveals that weight loss increases as the time of immersion, with the maximum of 8hrs at 303K. The result obtained showed that the inhibitor retarded the dissolution of Aluminum in 3 M KOH and 3 M NaOH solutions at all concentrations used, this agrees with the literature [20]. Furthermore, the results in Table 1 shows that the extracts work as good corrosion inhibitor for Aluminum in 3 M KOH and 3 M NaOH solutions since the corrosion rate was suppressed in the presence of the extract than in the absence. The Table also, indicates that the corrosion rate decreases as the concentration increases, but increases with the temperature up to 343K for the concentrations studied. Inhibition efficiency increases as the inhibitor concentration increases with the highest percentage at 80% for 3 M KOH compared to 75% for 3 M NaOH at same 303K and 1.0 g/L. Again, the Inhibition efficiency decreases as the temperature increases suggesting that the inhibitors were physically adsorbed on the surface of the metal, this is similar to other reports by [21].

Table1: Corrosion rate and Inhibition efficiency of D. *guineense* extract on Al corrosion in 3 M KOH and 3 M NaOH at different temperatures.

Conc	3 M KOH						3 M NaOH					
	CR (g cm^{-2} h^{-1})			η%			CR (g cm^{-2} h^{-1})			η%		
	303K	323K	343K	303K	323K	343K	303K	323K	343K	303K	323K	343K
0.0g/l	76	80	138				43	54	109			
0.2g/l	47	52	92	33	29	25	25	34	72	47	41	35
0.4g/l	40	46	86	40	37	40	19	26	64	51	49	40
0.6g/l	28	32	62	60	56	47	16	24	63	63	55	48
0.8g/l	26	30	60	67	62	50	15	22	61	73	59	56
1.0g/l	26	29	55	80	65	60	14	21	57	75	69	61

3.2 Adsorption isotherms and thermodynamics properties

It is a known fact that adsorption isotherms can be used to explain the interaction between the metal surface and the inhibitor. The degree of surface coverage, θ, was computed for the different concentrations of the extracts from weight loss measurements as follows: η% = θ x100, assuming a direct relationship between surface coverage and inhibition efficiency. The surface coverage values obtained were applied to various adsorption isotherm models and correlation coefficient (R^2) proved useful in determining the best isotherm fit Table 2. Temkin and Langmuir adsorption isotherms showed the best fit as shown in Figure 3 (a & b) respectively, and formulated as

$$\exp(-2a\theta) = KC \qquad (5a)$$

Where θ is the surface coverage, C is the inhibitor concentration, 'a' is the molecule interaction parameter determined from the slope of the plot in Fig 3 and K is the equilibrium constant of the adsorption-desorption process which indicates the binding power of the inhibitors to the Al surface.

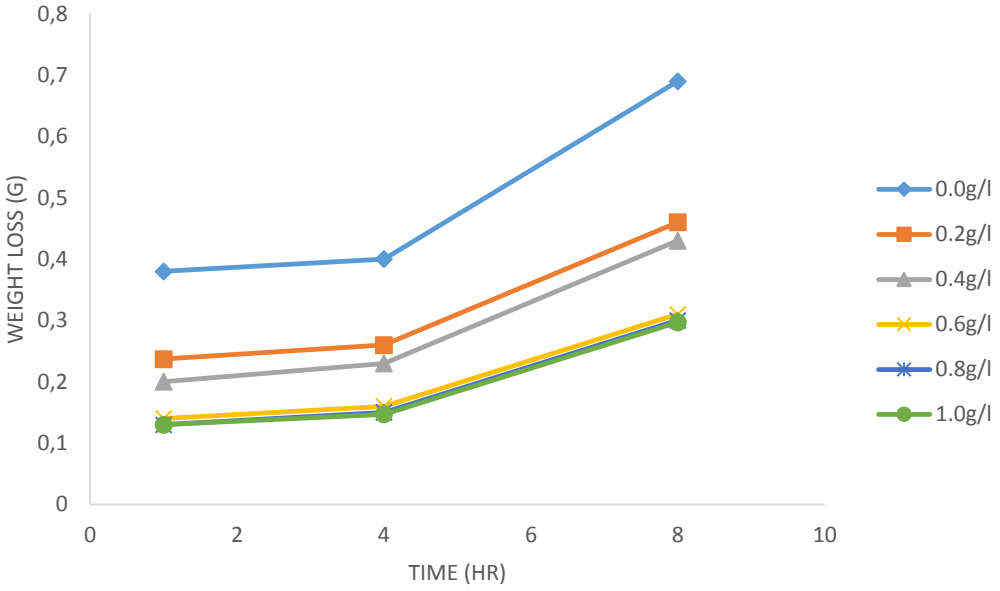

(a)

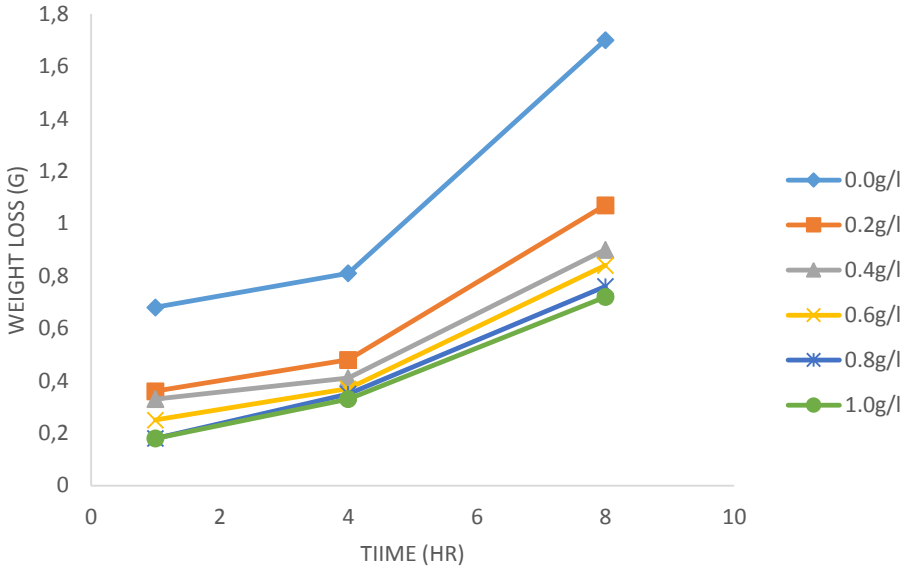

(b)

Figure 2: Plot of weight loss against time for Al in (a) 3 M KOH and (b) 3 M NaOH in the absence and presence of leaves extract of *D. guineense*.

The molecular interaction parameter can have either positive or negative values. The positive values show attractive forces between adsorbed molecules whereas negative values show repulsive forces between the adsorbed molecules [22]. The values of 'a' are all positive and it indicates that attraction exists in the adsorption layer. It also reveals that the attraction between molecules brings about an increase in the adsorption behavior and surface coverage [22]. Table 2 showed that Temkin adsorption isotherm performed better in 3 M KOH from the R^2 values while Langmuir adsorption isotherm also performed best with R^2 of 0.9999 at 303K in 3 M NaOH. The values of free energy of adsorption indicate that the inhibitors function by physically adsorbed on the metal surface. The values of free energy of adsorption up to -20 KJ/mol are consistent with electrostatic interaction between charged molecules and a charged metal (which indicates physical adsorption) while those more negative

than -40 KJ/mol involves charge sharing or transfer from the inhibitor molecules to the metal surface to form a coordinate type of bond (which indicates chemisorption). The values of free energy of adsorption obtained in this studied were dominated by physical adsorption of the extract on the surface of the metal at all temperatures [19].

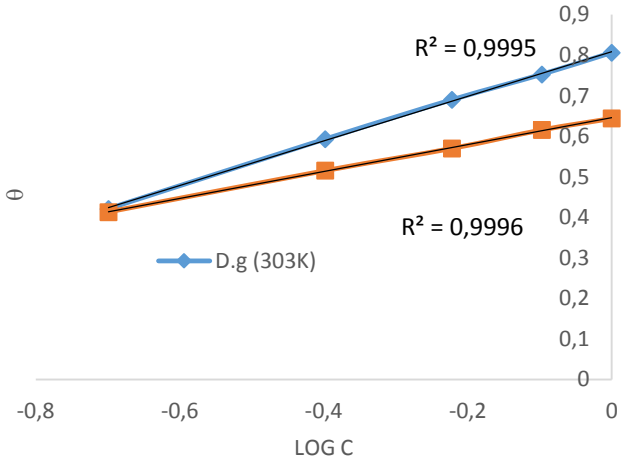

(a)

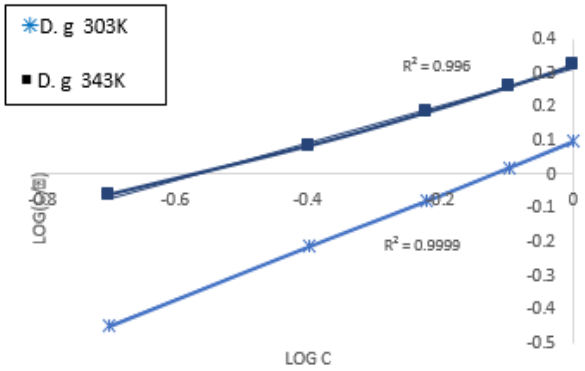

(b)

Figure 3: (a) Temkin adsorption isotherm plot for Aluminum in 3 M KOH and (b) Langumir adsorption isotherm plot for Aluminum in 3 M NaOH with D. *guineense* extracts at different temperatures.

Thermodynamic model is very useful in explaining the adsorption phenomenon of inhibitor molecule. The enthalpy of adsorption could be calculated according to the Van't Hoff equation [21].

$$lnK_{ads} = \frac{-\Delta H^{\circ}_{ads}}{RT} + constant \quad (5)$$

where $\triangle H^{\circ}_{ads}$ and K_{ads} are the enthalpies of adsorption and adsorptive equilibrium constant, respectively. The enthalpy of adsorption ($\triangle H$) can be approximately regarded as the standard enthalpy of adsorption $\triangle H^{\circ}_{ads}$ under the experimental conditions [13], [21] and the values obtained were all negative for both 3 M KOH and 3 M NaOH respectively. The standard adsorption free energy $\triangle G^{\circ}_{ads}$ listed in Table 2 were obtained using the relationship [3]:

$$logK_{ads} = -logC_{H_2O} - \frac{\Delta G^{\circ}_{ads}}{2.303RT} \quad (6)$$

Where C_{H_2O} is the concentration of water expressed in g/L (the same as that of inhibitor concentration), R is the molar gas constant and T is the absolute temperature. The standard Entropy of adsorption $\triangle S^{\circ}_{ads}$ was calculated from the fundamental thermodynamic equation shown in Eq. 7 and presented in Table 4:

$$\Delta G^{\circ}_{ads} = \Delta H^{\circ}_{ads} - T\Delta S^{\circ}_{ads} \quad (7)$$

Table 2: Temkin adsorption isotherm parameters for extracts of *D. guineense* at different temperatures

Adsorption Isotherm	Temperature (K)	R^2	Log K	K_{ads} (M^{-1})	Slope	ΔG_{ads} (kJ/mol)		Isotherm value
				3 M NaOH				
Temkin	303	0.9992	-1.8185	0.0152	0.599	0.4285	a	-0.724
Isotherm	343	0.9156	-2.3864	0.0041	0.2412	4.2223		-4.292
Langumir	303	0.9999	0.0940	1.2417	0.7761	-10.6651		
Isotherm	343	0.9960	0.3109	2.0460	0.5466	-13.4975		
				3 M KOH				
Temkin	303	0.9996	-0.7497	0.1780	0.5374	-5.7709		-1.068
Isotherm	343	0.9995	-1.9829	0.0104	0.3275	1.5674	a	-3.416
Langumir	303	0.9887	0.0809	1 .2048	0.595	-10.5890		
Isotherm	343	0.9897	0.1663	1.4666	0.6964	-12.547		

Valuable information on corrosion inhibition mechanism for adsorption of inhibitors on the surface of metals are provided by thermodynamic properties. The values of $\triangle G°_{ads}$ were all negative implying that the adsorption of *D. guineense* onto the Al surface was spontaneous [15] and strong interactions exist between the metal surface and the inhibitor molecules. In order to provide more insight into the thermodynamic properties, the values of $\triangle G_{ads}$ were plotted against T as shown in Figure 4. The slope of the straight line graph give the change in entropy of adsorption as can be seen in Eq.7 and enthalpy was computed from the intercept.

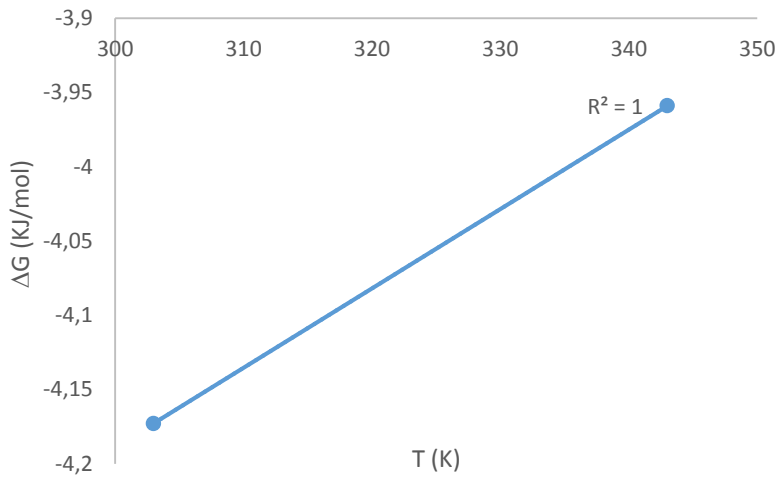

Figure 4: The relationship between $\triangle G°_{ads}$ and T

Figure 5 presents the linear plot of K_{ads} against I/T with ($\triangle H_{ads}/R$) as the slope and intercept of ($\triangle S/R$-ln55.5) [21]. Furthermore, Standard enthalpy of adsorption $\triangle H°_{ads}$ can also be calculated from the Gibbs–Helmholtz equation as presented in Eq. [8]

$$\frac{\Delta G°_{ads}}{T} = \frac{\Delta H°_{ads}}{T} + Constant \quad (8)$$

The calculated $\triangle H°_{ads}$ values using the Gibbs–Helmholtz and fundamental thermodynamic equations, are -33.1 and -21. 2 kJ/mol respectively confirming the exothermic behaviour of adsorption on the Al surface, therefore, the values of $\triangle H°_{ads}$, obtained by both methods are in good agreement. The exothermic adsorption process $\triangle H°_{ads} < 0$ imply either physisorption or chemisorption or a mixture of both processes while the endothermic adsorption process $\triangle H°_{ads} > 0$ implies chemisorption [5]. It can be seen from Table 3 that the positive sign of $\triangle H°_{ads}$ shows that the adsorption of molecules of the extracts is an exothermic process but the negative signs or values of $\triangle S°_{ads}$

indicate that the adsorption process is accompanied by a reduction in entropy [4]. Since the values of $\triangle S°_{ads}$ are all negative, it implies that the molecules of the extracts are adsorbed in an ordered manner on the Al surface, thereby causing a reduction in entropy [21].

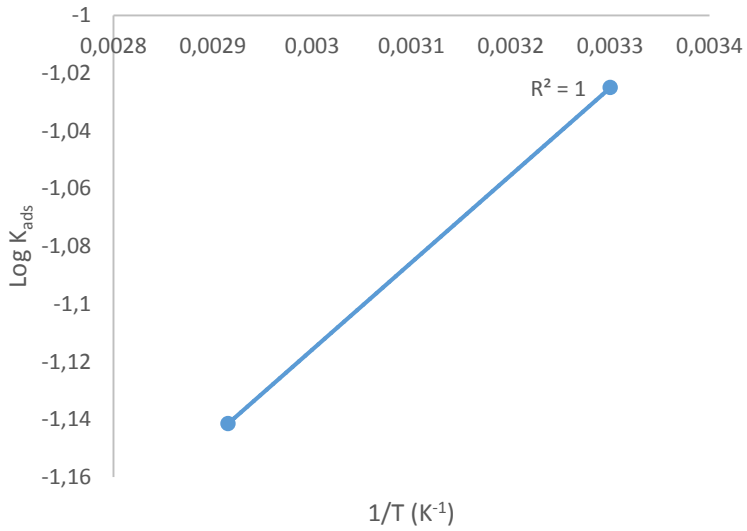

Figure 5: The relationship between $\ln K_{ads}$ and 1/T

3.3 Kinetic parameters

According to some authors [18], temperature has a great effect on the rate of metal electrochemical corrosion. The effect of temperature on the corrosion and inhibition process of Aluminum in 3 M KOH and 3 M NaOH in the absence and presence of different concentrations of the *D. guineense* extracts after 8hr of immersion was studied at 303, 323 and 343K using weight loss and electrochemical measurements.

The results of the effect of temperature on corrosion rate are presented in Table3 and in agreement with earlier reports of studies involving plant extracts [22] increasing as temperature increases. The dependence of corrosion rate on temperature can be expressed by the Arrhenius equation:

$$\log Cr = \log A - \left(\frac{E_a}{2.303RT}\right) \quad (9)$$

where Cr is the corrosion rate, Ea is the apparent activation energy of the Aluminum dissolution, R is the molar gas constant, T is the absolute temperature, and A is the frequency factor. Figure 6 depicts Arrhenius plot as log of corrosion rate (log Cr) against the reciprocal of temperature (1/T) for Aluminum in 3M KOH and 3 M NaOH in the free alkaline solutions and the alkaline containing different concentrations of *D. guineense* leaves extracts. The plots obtained are straight lines and the activation energy was evaluated from the slope of the straight line plots. The calculated values of activation energy are listed in Table 3. The values of activation energy, (E_a) are higher in the presence of the inhibitors than in their absence [12]. This observation agrees with the proposed physical adsorption mechanism. Also, Ea increases with increase in extracts concentration for both plant parts. Similar observation has been reported by [19] in their studies of the inhibition of corrosion of mild steel in hydrochloric acid solution by the extract of Kalmegh leaves extract.

The enthalpy, $\triangle H°$ and entropy, $\triangle S°$ of activation for the corrosion process, was calculated using the alternative Arrhenius equation, called transition state equations [23], was used:

$$log\left(\frac{C_r}{T}\right) = \left[\left(log\frac{R}{Nh}\right) + \left(\frac{\Delta S°}{2.303R}\right)\right] - \frac{\Delta H°}{2.303RT} \quad (10)$$

where h is the Planck's constant, N is the Avogadro's number, $\triangle S°$ is the entropy of activation, T is the absolute temperature and R is the universal gas constant.

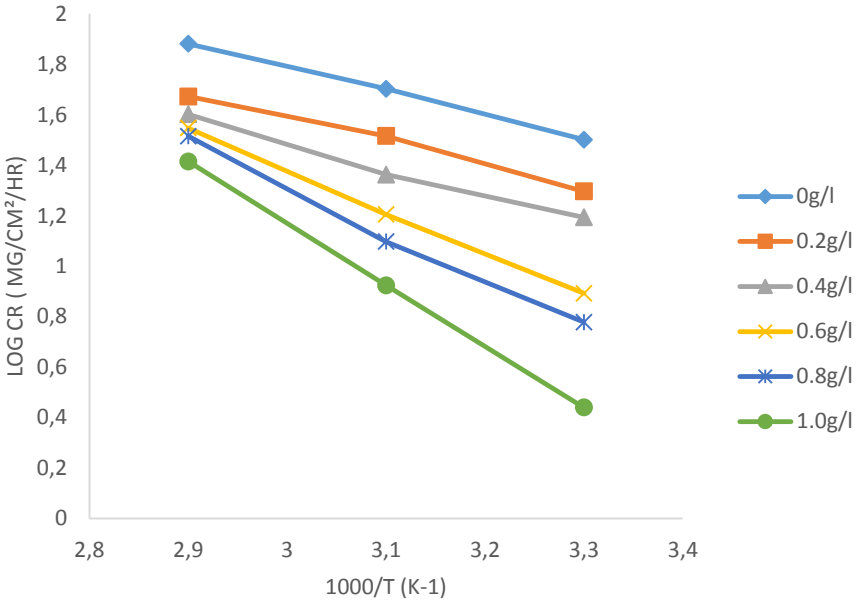

(a)

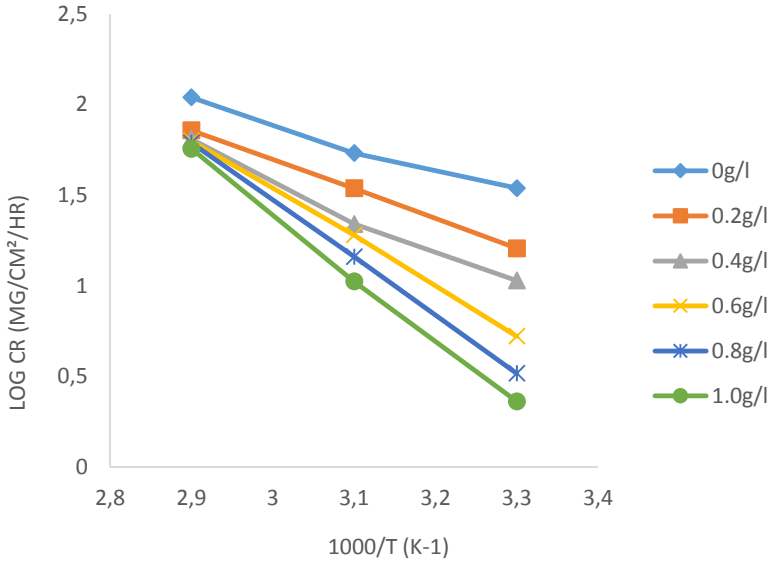

(b)

Figure 6: Arrhenius plot for Aluminum in (a) 3 M KOH and (b) 3 M NaOH with and without different concentrations of *D. guineense* extracts.

The linear plots of log(Cr/T) against 1/T deduced from Eq. (10) was applied in the computation of △H° and △S° from the slope of △H° = 2:303R and an intercept of (log(R/Nh) + △S°/2.303R) as shown in Figure 7 for extracts of *D. guineense* . The values of △H° and △S° are given in Table 3. The positive values of △H° both in the absence and presence of additives reflect the endothermic nature of the metal dissolution process [17]. The values of △S° in the absence and presence of the extracts are negative Table3. This indicates that the activated complex in the rate determining step represents an association rather than dissociation meaning that a decrease in disordering takes place on going from reactants to activated complex [15]. Also the △S° values tend to more negative values as the extract concentration increases showing more ordered behaviour leading to increase inhibition efficiency.

Heat of adsorption (Qads) was evaluated from the kinetic thermodynamic model to further gain insight into the adsorption mechanism using the expression [23].

$$Q_{ads} = 2.303R\left[\log\left(\frac{\theta_2}{1-\theta_2}\right) - log\left(\frac{\theta_1}{1-\theta_1}\right)\right]\frac{T_2T_1}{T_2-T_1} \quad (11)$$

where θ is the surface coverage, and T_1 and T_2 is the initial and final temperature (K), R is the universal gas constant. The values of heat of adsorption were obtained from Eq (11) but not shown. The values are negative and increases with increase in concentration of the extracts. Negative values of Q_{ads} (as obtained in this study) have been reported to indicate that the inhibitor adsorption and, hence, inhibition efficiency decreases with rise in temperature, while positive values mean the opposite effect [14]. The negative values of heat of adsorption obtained also support the physical adsorption mechanism.

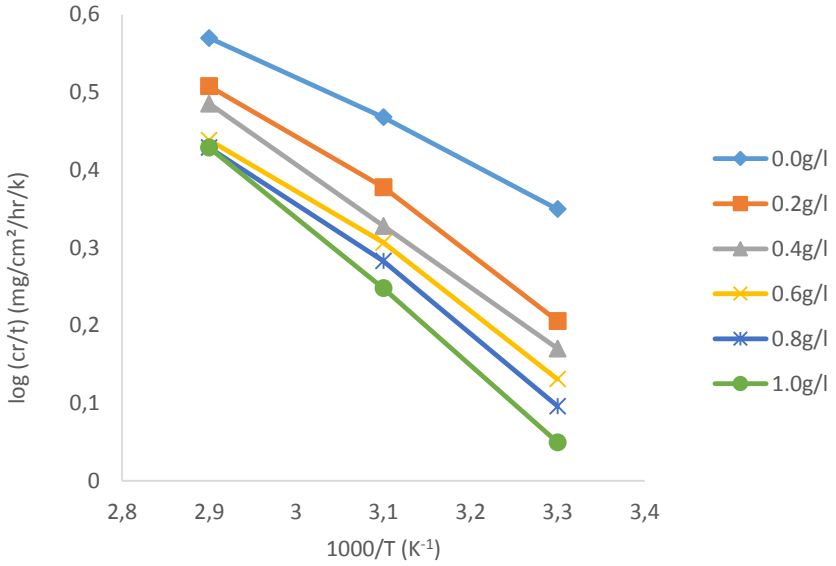

(a)

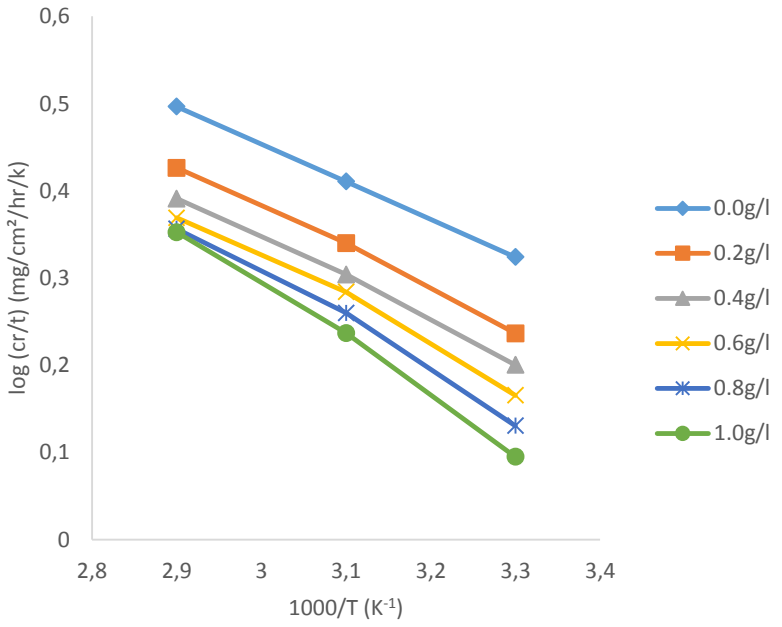

(b)

Figure 7: Transition state plot for aluminum in (a) 3 M KOH and (b) 3 M NaOH with and without different concentrations of *D. guineense* extracts.

Table 3: Activation parameters for Aluminum in 3 M KOH and 3 M NaOH in the absence and presence of different concentrations *D. guineense* extracts.

Conc.	Ea KJ/mol	ΔH KJ/mol	ΔS J/molK^{-1}	Ea (KJ/mol)	ΔH KJ/mol	ΔS JmolK^{-1}
0.0g/l	47.8	44.6	-40.6	50.7	51.7	-0.05
0.2g/l	56.2	53.8	-39.5	52.4	50.5	-0.08
0.4g/l	54.4	51.5	-48.4	56.6	53.4	-0.07
0.6g/l	50.1	48.0	-50.6	56.4	54.0	-0.07
0.8g/l	49.2	46.4	-48.7	59.5	55.7	-0.07
1.0g/l	49.6	44.5	-40.1	56.0	53/0	-0.06

3.4 Potentiodynamic *polarization study*

Figure 8 shows the polarization curves obtained from potentiodynamic polarization study for Al in the absence and presence of *D. guineense* extracts in 3 M KOH and 3 M NaOH respectively. The values of the polarization parameters are provided in Table 4 both were obtained from the extrapolation of the anodic and Cathodic Tafel slopes with respect to the E_{corr} values.

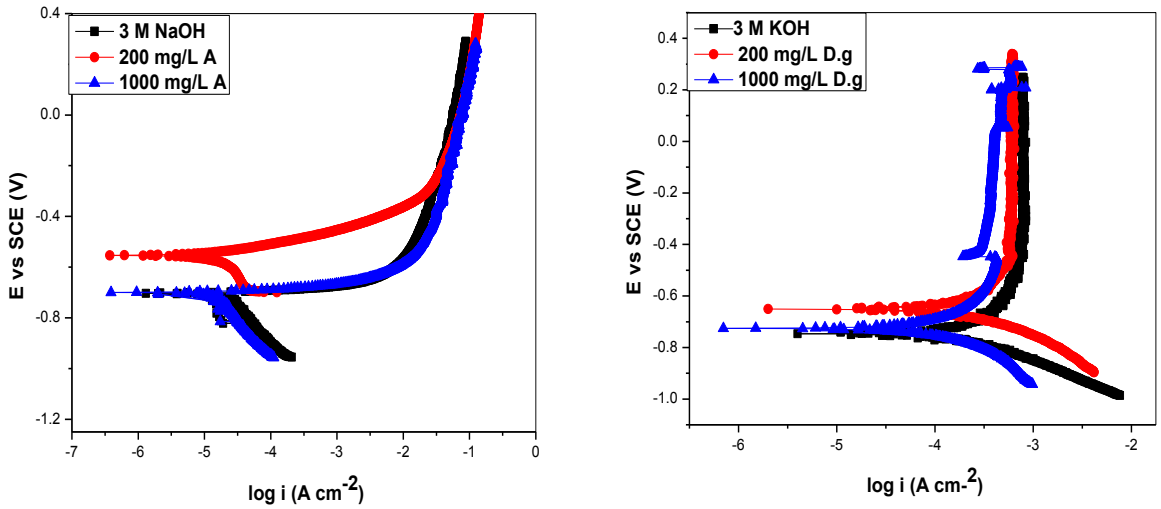

(a) (b)

Figure 8: polarization curve for Al in (a) 3 M KOH and (b) 3 M NaOH in the presence and absence of *D. guineense* extracts.

The values in Table 4 reveal that in the presence of *D. guineense* and at higher concentration of 1000 mg/L Al displayed lower i_{corr} and more positive E_{corr} values in the studied environments. In 3 M NaOH environment, (Figure 8a), the corrosion potential, E_{corr}, and the corresponding i_{corr} of Al in the absence and presence of *D. guineense* are presented in Table 4. The result shows that the introduction of *D. guineense* reduces both the cathodic and the anodic corrosion current densities, thus implying that the corrosion rate of Al sample in the presence of the inhibitor was reduced when compared to the uninhibited Al. Also, the E_{corr} of the inhibited Al is more positive (anodic) than the uninhibited Al especially in the presence of the inhibitor. This shows that in the absence of *D. guineense*, Al have a higher susceptibility to corrosion in this environment than the inhibited Al sample [24].

Table 4: Polarization parameters for Al in 3 M NaOH and 3 M KOH solution in the absence and presence of *D. guineense*.

System	E_{corr} (mV vs SCE)	I_{corr} (µA/cm^2)	IE%
3 M NaOH	- 636	182.6	
200 mg/L *D. g*	- 572	63.4	65.3
1000 mg/L *D. g*	- 624	28.1	84.6
3 M KOH	- 765	265.9	
200 mg/L *D. g*	- 692	98.7	62.9
1000 mg/L *D. g*	- 756	12.5	95.3

In 3 M KOH solution (Figure 8b), the corrosion potential E_{corr} for Al in the absence and presence of *D. guineense* Al are slightly more negative than the corrosion potential E_{corr} of the Al sample in 3 M NaOH solution. The corresponding current densities have been given in Table 4. It is evident that the *D. guineense* shifts both the anodic and cathodic curves to lower values of current densities. The Tafel polarization curves for the Al samples in both environments exhibit passivation behavior and do not differ in nature of transition from active to passive states. The similarity of the polarization curves of both the uninhibited and inhibited Al samples indicates that the mechanism of the corrosion of Al in the absence of the inhibitor did not changed even when *D. guineense* was introduced into the alkaline solutions [24].

3.5 Electrochemical impedance spectroscopy

Figure 9 (a- f) demonstrates a typical Nyquist, Bode phase angle and Bode modulus plots in the absence and presence of *D. guineense extracts.* It is observed that the shape of Nyquist and Bode plots shows a negligible difference in shape in the presence of the inhibitors but the diameter of semi- circles increases as the concentration of the inhibitor increases. The values of R_s, R_ct and $C_{dl,}$ inhibition efficiency were calculated and presented in Table 5.

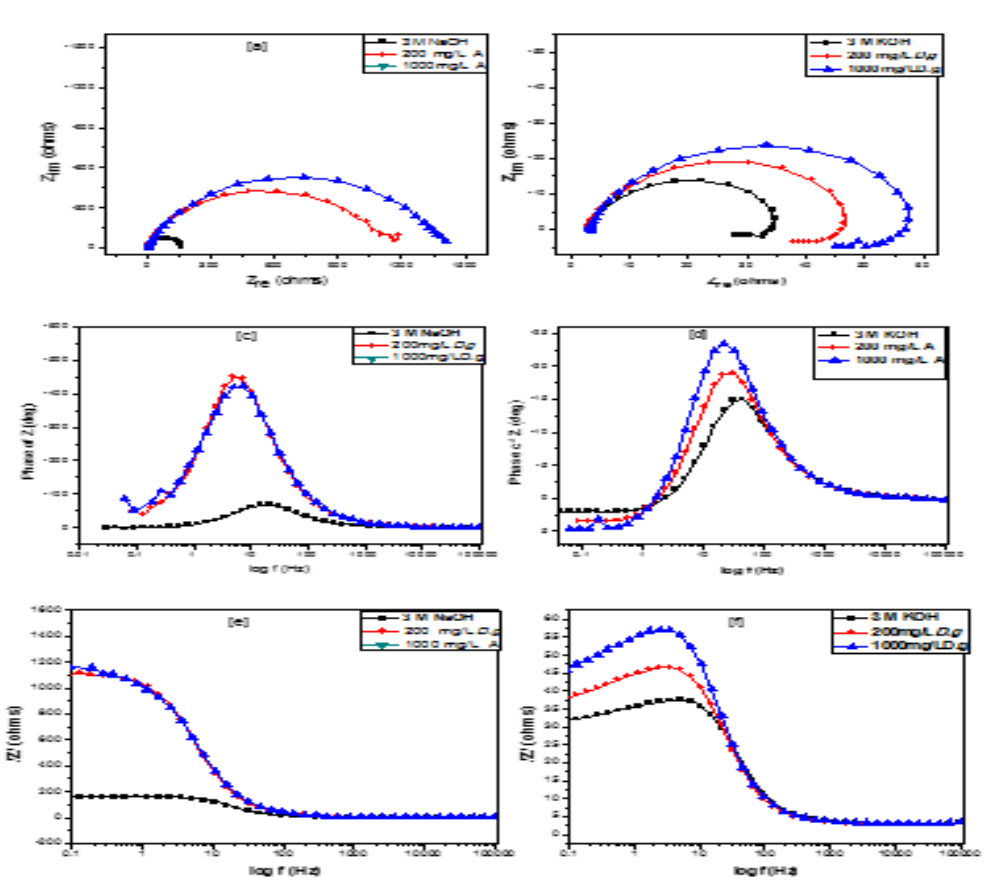

Figure 9(a-f): Electrochemical impedance plot for aluminum in 3 M NaOH and 3 M KOH respectively in the presence and absence of *D. guineense*; (a&b) Nyquist, (c &d) phase angles and (e &f) Bode modulus plots.

The Nyquist plots showed a capacitive loop followed by an inductive loop for the Al samples in 3 M NaOH and 3 M KOH solutions as shown in Fig 9(a - f). The diameter of the semi circles are related to charge transfer resistance. The size of the capacitive loops was greater in the presence of *D. guineense*, compared to that in the absence of the inhibitor; an indication of a higher corrosion resistance for Al in the presence of *D. guineense* [25]. The occurrence of an inductive loop in 3 M KOH solution solutions may indicate certain non – faradaic processes, such as adsorption and desorption of corrosion products, occurring at the sample / electrolyte interface. The equivalent circuit model shown in Figure1 was used to model the impedance results obtained for Al in 3 M KOH environment, after fitting with Zsimpwin software.

Table 5: Electrochemical parameters for Al in uninhibited and inhibited 3 M NaOH and 3 M KOH solutions

System	R_s (Ωcm^2)	R_{L1} (Ωcm^2)	R_{ct} (Ωcm^2)	C_{dl} (μFcm^2)	IE%
3 M NaOH	2.13	6.2	145.8	3.12	
200 mg/L *D.g*	3.72	532	1050.7	2.53	86.1
1000 mg/L D.g	3.98	1879	1418.2	2.12	89.7
3 M KOH	2.06	7.6	30.2	3.62	
200 mg/L *D.g*	2.67	32	47.4	3.64	36.3
1000 mg/L *D.g*	3.22	68	59.5	2.93	50.2

D.g = Dialium guineense

The inductance, L, and charge transfer resistance, (R_{ct}) characterize the processes beneath the store of charges. The result shows that the C_{dl} value was lower in the inhibited environment compared to the uninhibited solution. Similarly, the value of inductance was greater for the inhibited Al sample than for the uninhibited. It may indicate that introduction of *D. guineense* can modify the electrochemistry of the Al sample by reducing the penetrations of electrolyte into the substrate–electrolyte interface, thus, decreasing the rate of the corrosion in the alkaline solutions. This can also be evidenced by the higher value of R_{ct}, Table 5 for Al in the presence of the inhibitor than the value obtained in the absence of *D. guineense*. This is in line with [25].

It has been stated earlier that Al surfaces can form a protective layer of Al_2O_3 when in contact with aqueous solutions, this layer in question can characteristically lower the rate of the electrochemical corrosion on the Al surface. However, in the presence of *D. guineense*, its species adsorbs on the surface of Al, this creates a strong barrier between the Al surface and the electrolyte solutions. Again, addition of inhibitor also reduces the rate of penetration of the electrolyte. The presented result see Table 5 shows clearly that the introduction of *D. guineense* in both environments seem to reduce the susceptibility of the Al substrate to dissolution and to the electrochemical processes occurring at the substrate/electrolyte interface [26].

Finally one may conclude that the adsorption of *D. guineense* species serve as a barrier blocking the contact between the Al surface and the aggressive solutions. Furthermore, Figure 9(c & d) shows the Bode phase angle plots with one time constant. Figure 9(e & f) depicts clearly Bode modulus plots. Since the EIS results are in good agreement with potentiodynamic results, it implies that *D. guineense* performed well as a corrosion inhibitor for Aluminum in 3 M NaOH and 3 M KOH studied.

Due to the fact that corrosion reaction is basically an electrochemical process, the inhibiting effect of D. guineense (at low and high concentrations) were further investigated from an electrochemical perception. 200 mg/L and 1000 mg/L of D. guineense concentrations were used to show the nature of the inhibiting effect at low and high concentrations, respectively. Figure 10 (a & b) depicted the open circuit potential (EOCP) with time for aluminum in 3 M NaOH and 3 M KOH solution in the absence and presence of (200 mg/L and 1000 mg/L) D. guineense. The plots show some adjustments in the EOCP–time behavior as a result of the presence of D. guineense. A shift on anodic direction of EOCP was observed on addition of D. guineense in 3 M NaOH. The plot of EOCP–time in 3 M KOH indicate a distinctive differences in the shifts at low and high D. guineense concentrations. In the 3 M KOH (1000 mg/L) the EOCP values were more positive while in 3 M NaOH (200 mg/L) the achieved potential values were always more negative (cathodic) than the values in uninhibited. This in line with [27, 28].

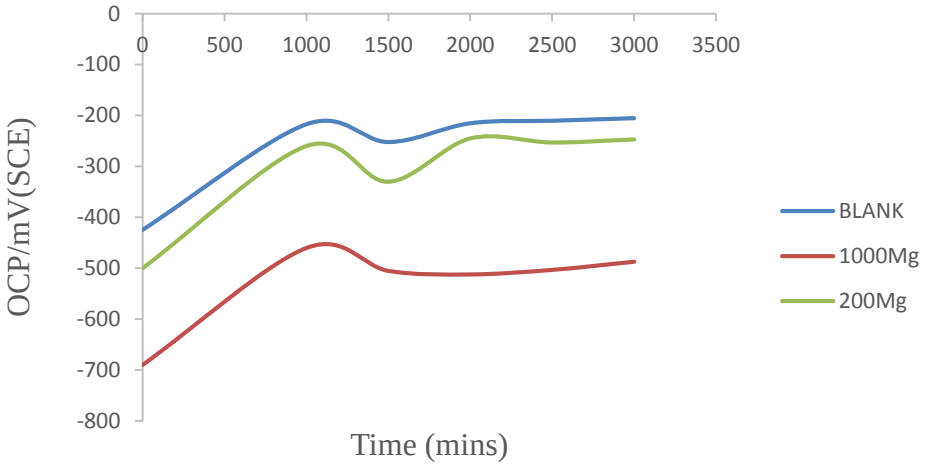

(a)

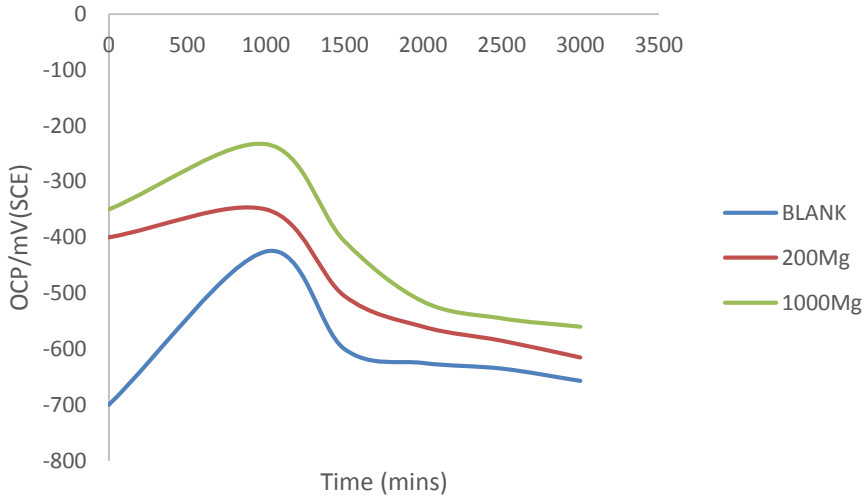

(b)

Figure 10 (a & b) : Open circuit potential (EOCP) with time for aluminum in 3 M NaOH and 3 M KOH solution in the absence and presence of (200 mg/L and 1000 mg/L) D.

Conclusion

In this study, inhibitive performance of *Dialium guineense* for Aluminum in 3 M NaOH and 3 M KOH has been studied and arrived at these results:

1. *Dialium guineense* leaf extract showed excellent inhibitive action against Aluminum in 3 M NaOH and 3 M KOH such that increase in the inhibitor concentration causes a remarkable improvements on their efficiencies.
2. The adsorption of *Dialium guineense* leaf extract on Al surface obeys Temkin adsorption isotherm model. Physical adsorption mechanism is proposed from the activation and thermodynamic parameters obtained.
3. There was good agreement between the data obtained from weight loss and electrochemical methods.
4. Potentiodynamic polarization measurements indicate that the *Dialium guineense* leaf extract acts as a mixed-type inhibitor.
5. Impedance considerations show that increasing the inhibitor concentrations increases the solution resistance considerably in all concentrations studied.

References

1. Al-Otaibi, M.S., Al- Mayouf, A.M., Khan, M., Mousa, A.A., Al-Mazroa, S.A., and Alkhathlan, H.Z., Corrosion inhibitory action of some plant extracts on the corrosion of mild steel in acidic media. *Arabian Journal of chemistry*, 7 (2014) 340-346.
2. Aprael, S. Yaro, Anes A. Khadom, and Rafal, K. Wael, Apricot juice as green corrosion inhibitor of mild steel in phosphoric acid. Alexandria Engineering Journal, Alexandria University, 52, 2013, 129-135.
3. Ehteram A. Noor, Potential of aqueous extract of Hibiscus sabdariffa leaves for inhibiting the corrosion of aluminum in alkaline solutions. J. Appl Electrochem, 39; 2009, 1465-1475, DOI10.1007/s10800-009-9826-I
4. Nnanna, Lebe A., John Wisdom O., and Nwadiuko Onyinyechi, corrosion inhibition study aluminum alloy AA3003 in alkaline medium by palisota hirsute extract. International Journal of Engineering Research and Reviews**,** 2,(4), 2014, 113-118
5. Ating, E.I., Umoren, S.A., Udousoro, I.I., Ebenso, E.E., and Udoh, A.P., Leaves extract of Ananas sativum as a green corrosion inhibitor for aluminum in hydrochloric acid solutions. Green chemistry Letters and Reviews, 3(2), 2010, 61-68.
6. QiBo, Zhang and YiXin, Hua, corrosion inhibition of aluminum in hydrochloric acid by alkylimidazolium ionic liquids. Materials chemistry and physics, Elsevier, 119, 2010, 57-64
7. Fouda, A.S., Shalabi, K., Mohamed, N. H., corrosion inhibition of aluminum in hydrochloric acid solutions using some Chalone derivatives. International journal of Innovative research in Science, Engineering and Technology, 3(3), 2014, 9861- 9875
8. Eno E. Ebenso and Ime B. Obot, Inhibitive properties, thermodynamic characterization and Quantum chemical studies of secnidazole on mild steel corrosion in acidic media. 5, 2010, 2012-2035.
9. Fouda, Abd El-Aziz S., Ahmed, Abdel Nazeer, Mohamed, Ibraim, and Mohammed, Fakih, Ginger Extract as a green corrosion inhibition for steel in sulfide polluted salt water. Journal of the Korean chemical society, 57(2), 2013, 272- 278
10. Leelavathi, S. and Rajalakshmi, R., Dodonaea viscosa (L.) leaves extract as acid corrosion inhibitor for mild steel-A green approach. J.Mater. Environ. Sci. 4(5), 2013, 625-638.
11. James, A. O. and Akaranta, O. the inhibition of corrosion of Zinc in 2.0M hydrochloric acid solution with acetone extract of red onion skin. African journal of pure and applied Chemistry, 3(11), 2009, 212 -217
12. Hui Cang, Zhenghao Fei, Hairong Xiao, Jiali, Huang and Qi Xu, Inhibition effect of Reed leaves extract on steel in hydrochloric acid and sulphuric acid solutions. Int. J. Electrochem Sci. 7, 2012, 8869 -8882
13. Okeoma Kelechukwu B., Computational and experimental studies on the inhibitive effects of newbouldia laevis extract and magnetic fields on copper corrosion in aqueous acidic media. International Letters of chemistry, physics and Astronomy, 54, 2015, 135 -142.
14. Ikeuba, A. I., Okafor, P.C U., Ekpe , J., and Eno, E. Ebenso, Alkaloid and non-alkaloid ethanolic extracts from seeds of Garcinia kola as green corrosion inhibitors of mild steel in H_2S0_4 solution. Int. J. Electrochem.Sci., 8, 2013, 7455-7467
15. Obot, I.B., and Obi-Egbedi, N.O., Ginseng root: A new efficient and effective Eco-friendly corrosion inhibitor for aluminum alloy of type AA1060 hydrochloric acid solution. *Int. J. Electrochem. Sci.*, 4 (2009) 1277 -1288
16 Oguzie, Emeka E., corrosion inhibitive effect and adsorption behaviour of Hibiscus sabdariffa extract on mild steel in acidic media. Portugaliae Electrochimica ACTA, 26, 2008, 303 -314
17. Nnanna, L. A., Obasi, V.U., Nwadiuko, O.C., Mejeh, K. I.., Ekekwe, N.D., and Udensi, S.C., Inhibition by newbouldia laevis leaf extract of corrosion of aluminum in HCL and H_2S0_4 solutions. 2012
18. Patel, N. S., Hrdlicka, J., Beranek, P., Pribyl, M., Snita, D., Hammouti, B., Al-Deyab, S. S., and Salghi, R., extract of phyllanthus fraternus leaves as corrosion inhibitor for mild steel in H_2S0_4 solutions. Int. J. Electrochem. Sci., 9, 2014, 2805-2815

19. Oguzie, Emeka E., Oguzie, Kanayo L., Akalezi, Chris O., Udeze, Irene O., Ogbulie, Jude N., and Njoku,Victor O., Natural products for materials protection: corrosion and microbial growth inhibition using capsicum frutescens biomass extracts. ACS Sustainable Chem. Eng, 1, 2012, 214 -225

20. Ejikeme, P.M., Umana, S.G., and Onukwuli, O. D., corrosion inhibitor for aluminum by treculia Africana leaves extract in acidic medium. Portugaliae Electrochimica Acta, 30(5), 2012, 317- 328

21. Umoren, S. A., Eduok, U. M., Solomon M. M., and Udoh, A. P., corrosion inhibition by leaves and stem extracts of sida acuta for mild steel in 1M H_2SO_4 solutions investigated by chemical and spectroscopic techniques, Arabian Journal of chemistry, King Saudi University, 201

22. Okafor, P. C., Eno E. Ebenso, and Udofot J. Ekpe, Azdirachta indica extracts as corrosion inhibitor for mild stein acid medium. Int. J. Electrochem. Sci.5, 2010, 978- 993.

23. Ezeoke, Acha U., Adeyemi, Olalere G., Akerele, Opeyemi A., and Obi-Egbedi, Nelson O., Computational and experimental studies of 4-Aminoantipyrine as corrosion inhibitor for mild steel in sulphuric acid solution. Int. J. Electrochem. Sci. 7, 2012, 534-553

24. Helal, N.H., El-Rabiee, M.. M., Abd El-Hafez, G. M., Badawya, W.A., Environmentally safe corrosion inhibition of Pb in aqueous solutions. Journal of Alloys and Compounds. 45(6), 2008, 372–378

25. Fan, Zhang Yongming, Tang, Ziyi Cao, Wenheng, Jing Zhenglei, Wu, Yizhong Chen, Performance and theoretical study on corrosion inhibition of 2-(4-pyridyl) benzimidazole for mild steel in hydrochloric acid. corrosion science 2012.

26. Pandian, Bothi Raja, Afidah, Abdul Rahim, Hasnah, Osman, and Khalijah Awang, Inhibitive effect of *Xylopia ferruginea* extract on the corrosion ofmild steel in 1M HCl medium. I*nternational Journal of Minerals, Metallurgy and Materials*, *18(4)*, 2011 *Page 413;* DOI: 10.1007/s12613-011-0455-4

27. Oguzie, E.E., Enenebeaku, C.K., Akalezi, C.O., Okoro,, S.C. Ayuk, A.A. and Ejike, E.N., Adsorption and corrosion-inhibiting effect of Dacryodis edulis extract on low-carbon-steel corrosion in acidic media, Journal of Colloid and Interface Science 349 (2010) 283–292.

28 Sayed S. Abdel Rehim, Omar A. Hazzazi, Mohammed A. Amin, Khaled F. Khaled, On the corrosion inhibition of low carbon steel in concentrated sulphuric acid solutions. Part I: Chemical and electrochemical (AC and DC) studies, Corrosion Science 50 (2008) 2258–2271.